A Density Functional Study of β-Hydride and Methyl Migratory Insertion in $CpM(PH_3)(CH_2CH_2)R^+$ (M = Co, Rh, Ir; R = H, CH_3)

Yunzhu Han, Liqun Deng, and Tom Ziegler*

Contribution from the Department of Chemistry, University of Calgary, Calgary, Alberta, Canada T2N 1N4

Received January 2, 1997. Revised Manuscript Received March 31, 1997[⊗]

Abstract: The hydride and methyl β-migratory insertion processes in $CpM(PH_3)(CH_2CH_2)R^+$ (M = Co, Rh, Ir; R = H, CH_3) as well as the microscopically reverse β-elimination reactions have been studied by relativistic density functional theory. The calculations reveal that the β-migratory insertion reactions of the olefin hydride complexes $CpM(PH_3)(CH_2CH_2)H^+$ (M = Co, Rh, Ir) have electronic reaction barriers of 0.3 (Co), 2.7 (Rh), and 6.1 kcal/mol (Ir), respectively. Further, the β-migratory insertion reactions of hydride are exothermic for cobalt ($\Delta H_e = -3.4$ kcal/mol) and rhodium ($\Delta H_e = -1.0$ kcal/mol), but endothermic for iridium ($\Delta H_e = 3.7$ kcal/mol). Relativistic effects are important for the calculated trends within the cobalt triad. Without relativity the β-migratory insertion reactions would be exothermic for all three metals. For the corresponding β-migratory insertion reactions of methyl the barriers are 15.2 (Co), 19.8 (Rh), and 23.2 kcal/mol (Ir), respectively. The reactions are exothermic for all three metals with $\Delta H_e = -12.7$ (Co), -8.5 (Rh), and -5.3 kcal/mol (Ir), respectively. Structures of reactants, transition states, and products were fully optimized. For the hydride migration, the transition states are close to the hydrido olefin systems $CpM(PH_3)(CH_2CH_2)H^+$ for M = Co and Rh, whereas the transition states for the iridium hydride resemble the ethyl compound $CpIr(PH_3)(CH_2CH_2H)^+$. The transition states for the methyl migration are product-like for all three metals. The most stable conformation of the ethyl and propyl product complexes $CpM(PH_3)(CH_2CH_2R)^+$ exhibits in all cases a β-agostic M−H−C interaction. The strength of this interaction decreases down the cobalt triad. An extensive thermochemical analysis is provided for the relative stability of $CpM(PH_3)(CH_2CH_2)R^+$ and $CpM(PH_3)(CH_2CH_2R)^+$ (M = Co, Rh, Ir; R = H, CH_3).

Introduction

The β-hydride and methyl elimination processes in transition metal alkyls as well as the microscopically reversible β-migratory insertion reactions, eqs 1 and 2, are fundamental transformations of importance in many catalytic processes, including olefin hydrogenations, hydroformylations, isomerizations, olefin polymerizations, and related oligomerizations and dimerizations.[1−4]

Given the importance of β-migratory insertion and β-elimination processes, it is quite understandable that these reactions have been studied extensively. Experimental[1,3,4] and theoretical[2] studies to date indicate that the β-migratory aptitude of hydride is higher than that of alkyl. Also, the migratory insertion barriers appear to be much smaller for early transition metals[2g,i−k,3a] with a d^0 configuration than for late transition metals[2e,f,2h,l,3d,4] with d^6 or d^8 configurations, at least in the case of alkyl migration. Further, the alkyl complexes are more stable than the corresponding olefin hydrido[2m,3e,f] or alkyl isomers[2k,e,f] for early transition metals, whereas the equilibrium might shift toward the olefin hydrido[4] or alkyl isomers for late transition metals. However, the available experimental data in support of the above trends are still limited and in many cases indirect.

We shall here study the two processes given in eqs 1 and 2 for the late transition metals cobalt, rhodium, and iridium with a d^6 configuration. Our objective has been to estimate the energies of the olefin hydrido, **1**, and olefin methyl, **4**, systems relative to their respective alkyl isomers **2** and **5**. In addition, attention will be given to the barriers of activation for the two processes and the nature of the transition states **TS1** and **TS2** as well as the resulting alkyl products **2**, **3** and **5**, **6**. Finally the study of all three members of the cobalt triad allows us to probe any periodic trend in the relative migratory aptitude of hydride compared to methyl. This investigation has been

* Author to whom all correspondence should be addressed.

[⊗] Abstract published in *Advance ACS Abstracts,* June 1, 1997.

(1) (a) Crabtree, R. H. *The Organometallic Chemistry of Transition Metals*; John Wiley & Sons: New York, 1988. (b) Yamamoto, A. *Organotransition Metal Chemistry*; John Wiley & Sons: New York, 1986. (c) Collman, J. P.; Hegedus, L. S.; Norton, J. R.; Finke, R. G. *Principles and Applications of Organotransition Metal Chemistry*; University Science Books: Mill Valley, CA, 1987.

(2) (a) Musaev, D. G.; Morokuma, K. *Adv. Chem. Phys*. **1996**, *95*, 61. (b) Leeuwen, v. P. W. N. M.; Morokuma, K.; Lenthe v. J. H., Eds. In *Theoretical Aspects of Homogeneous Catalysis*; Kluwer Academic Publishers: Dordrecht, 1995. (c) Yosida, S.; Sakaki, S.; Kobayashi, H. *Electronic Processes in Catalysis*; VCH: New York, 1994. (d) Dedieu, A., Ed. *Transition Metal Hydrides*; VCH Publishers: New York, 1994. (e) Koga, N.; Morokuma, K. *Chem. Rev.* **1991**, *91*, 823. (f) Siegbahn, P. E. M. *J. Am. Chem. Soc.* **1993**, *115*, 5803. (g) Lauher, J. W.; Hoffmann, R. *J. Am. Chem. Soc*. **1976**, *98*, 1729. (h) Thorn, D. L.; Hoffmann, R. *J. Am. Chem. Soc.* **1978**, *100*, 2079. (i) Weiss, H.; Enrig, M.; Ahlrich, R. *J. Am. Chem. Soc*. **1994**, *116*, 4919. (j) Woo, T. K.; Fan, L.; Ziegler, T. *Organometallics* **1994**, *13*, 432. (k) Margl, P.; Lohrenz, J. C. W.; Ziegler, T.; Bloechl, P. E. *J. Am. Chem. Soc.* **1996**, *118*, 4434. (l) Margl, P.; Ziegler, T. *J. Am. Chem. Soc.* **1996**, *118*, 7337. (m) Ziegler, T.; Folga, E.; Berces, A. *J. Am. Chem. Soc.* **1993**, *115*, 1289.

(3) (a) Lin, Z.; Marks, T. *J. Am. Chem. Soc.* **1990**, *112*, 5515. (b) Johnson, L. K.; Mecking, S.; Brookhart, M. *J. Am. Chem. Soc.* **1996**, *118*, 267. (c) Johnson, L. K.; Killian, C. M.; Brookhart, M. *J. Am. Chem. Soc.* **1995**, *117*, 6414. (d) Rix, F. C.; Brookhart, M.; White, P. S. *J. Am. Chem. Soc.* **1996**, *118*, 4746. (e) Watson, P. L. In *Selective Hydrocarbon Activation*; Davis, J. A., Watson, P. L., Liebman, J. F., Greenberg, A., Eds.; VCH Publishers: New York, 1990. (f) Burger, B. J.; Thompson, M. E.; Cotter, W. D.; Bercaw, J. E. *J. Am. Chem. Soc.* **1990**, *112*, 1566. (g) Richardson, D. E.; Alameddin, N. G.; Ryan, M. F.; Hayes, T.; Eyler, J. R.; Siedle, A. R. *J. Am. Chem. Soc.* **1996**, *118*, 11244.

(4) (a) Brookhart, M.; Hauptman, E.; Lincoln, D. M. *J. Am. Chem. Soc.* **1992**, *114*, 10394. (b) Brookhart, M.; Lincoln, D. M. *J. Am. Chem. Soc.* **1988**, *110*, 8719. (c) Brookhart, M.; Volpe, A. F.; Lincoln, D. M.; Horvath, I. T.; Miller, J. M. *J. Am. Chem. Soc*. **1990**, *112*, 5634.

S0002-7863(97)00015-2 CCC: $14.00

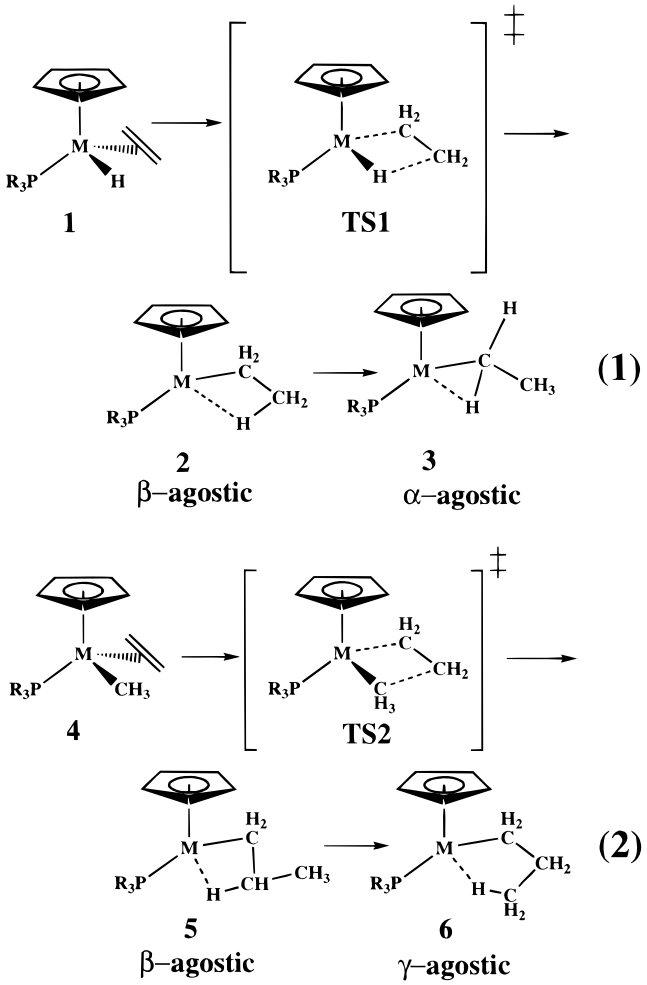

prompted by recent studies by Brookhart et al.[4] in which some of the same objectives mentioned here were initially addressed experimentally.

Computational Details

All calculations in this study were carried out by using the Amsterdam density functional package, ADF, developed by Baerends et al.,[5] and vectorized by Ravenek.[6] The adopted numerical integration scheme applied for the calculations was developed by te Velde et al.[7] A set of uncontracted triple-ζ Slater-type orbitals (STO) was employed for the *n*s, *n*p, *n*d, $(n + 1)$s, and $(n + 1)$p valence shells of the transition metal atoms. A double-ζ STO basis set was used for carbon (2s, 2p), hydrogen (1s), and phosphorus (3s, 3p). A single 3d STO polarization function was employed for carbon and phosphorus whereas a 2p STO function was added to hydrogen. The inner core shells were treated by the frozen-core approximation.[5] A set of auxiliary s, p, d, f, and g STO functions, centered on all nuclei, was introduced to fit the molecular density and to present Coulomb and exchange potentials accurately in each SCF cycle.[8] All geometries were optimized with the local density approximation (LDA)[9] and the analytical energy gradient scheme proposed by Verslius and Ziegler.[10] Energy differences were calculated by augmenting the local exchange-correlation energy expression from Vosko et al.[11] with Becke's nonlocal exchange correction[12] and Perdew's nonlocal correlation correction.[13] The transition states were located with the algorithm given by Baker.[14]

The extended transition state (ETS) method[15] was applied to analyze the bond energies. The ETS method decomposes the bond energy, BE, between fragments A and B in the AB molecule as

$$\mathrm{BE} = -[\Delta E_{\mathrm{steric}} + \Delta E_{\mathrm{orbit}} + \Delta E_{\mathrm{prep}}] \tag{3}$$

On the right-hand side of eq 3, the first term is the steric interaction energy between A and B. It can be written as

$$\Delta E_{\mathrm{steric}} = \Delta E_{\mathrm{el}} + \Delta E_{\mathrm{Pauli}} \tag{4}$$

where ΔE_{el} is the electrostatic Coulomb interaction between A and B, whereas $\Delta E_{\mathrm{Pauli}}$ is the Pauli repulsion due to the destablizing two-orbital four-electron interactions between occupied orbitals on A and B. The term $\Delta E_{\mathrm{orbit}}$ represents the stabilizing interaction between occupied and virtual orbitals on A and B, and ΔE_{prep} takes into account geometrical deformations of A and B as the two fragments are combined into A−B. Relativistic effects were taken into account by the method given by Snijders et al.[16] based on first-order perturbation theory. The perturbative method used here for nonlocal and relativistic effects has been validated by Li et al.[17] It was shown by Li et al. that the perturbative approach affords energies and structures similar to those obtained by a procedure in which nonlocal and relativistic effects are treated self-consistently.

Results and Discussion

Structures. We have been able to locate two stable key structures on the potential energy surface for the *β*-migratory insertion of ethylene into the metal−hydrogen bond, eq 1. The first, **1**, represents the hydrido olefin reactant of eq 1, and the second, **2**, the resulting ethyl complex with a pronounced *β*-agostic M−H−C interaction of eq 1. The optimized geometries (key parameters) of **1** and **2** are given in Table 1. The agostic interaction for the three-center two-electron C−H−M bonds in the ethyl product **2** is marked clearly by elongated C−H distances (*g*) of 1.267, 1.248, and 1.236 Å for Co, Rh, and Ir, respectively. We note further the presence of partially retained C−C double bonds with distances (*d*) of 1.450 (Co), 1.449 (Rh), and 1.455 Å (Ir). These distances are only 0.05 Å longer than the corresponding C−C double bonds of the olefin hydrido reactants, **1**, at 1.395 (Co), 1.391 (Rh), and 1.394 Å (Ir), respectively. Further, the *β*-agostic ethyl products have close M−H contacts at 1.58 (Co), 1.70 (Rh), and 1.80 Å (Ir). They are not substantially longer than the M−H bonds of the olefin hydrido reactants, **1**, at 1.45 (Co), 1.58 (Rh), and 1.59 Å (Ir), respectively. Structures of hydrido olefin complexes involving the cobalt triad are not known. However, the optimized M−H and C−C distances are quite representative

(5) (a) Baerends, E. J.; Ellis, D. E.; Ros, P. *Chem. Phys.* **1973**, *2*, 41. (b) Fonseca, C.; Visser, O.; Snijders, J. G.; te Velde, G.; Baerends, E. J. In *Methods and Techniques in Computational Chemistry*; METECC-95; Clementi, E.; Corongiu, G., Eds.; Cagliari, 1995; p 307.

(6) Ravenek, W. In *Algorithms and Applications on Vector and Parallel Computers*; te Riele, H. J. J., Dekker, T. J., van de Vorst, H. A., Eds.; Elsevier: Amsterdam, 1987.

(7) (a) Boerrigter, P. M.; te Velde, G.; Baerends, E. J. *Int. J. Quantum Chem.* **1988**, *33*, 87. (b) te Velde, G.; Baerends, E. J. *J. Comput. Phys.* **1992**, *99*, 84.

(8) Krijn, J.; Baerends, E. J. Fit functions in the HFS-method; Internal report (in Dutch); Free University of Amsterdam, The Netherlands, 1984.

(9) Gunnarson, O.; Lundquist, I. *Phys. Rev.* **1974**, *10*, 1319.

(10) Verluis, L.; Ziegler, T. *J. Chem. Phys.* **1988**, *88*, 322.

(11) Vosko, S. H.; Wilk, L.; Nusair, M. *Can. J. Phys.* **1980**, *58*, 1200.

(12) Becke, A. D. *Phys. Rev. A* **1988**, *38*, 2398.

(13) (a) Perdew, J. P. *Phys. Rev. Lett.* **1985**, *55*, 1655. (b) Perdew, J. P. *Phys. Rev. B* **1986**, *33*, 8822. (c) Perdew, J. P.; Wang, Y. *Phys. Rev. B* **1986**, *33*, 8800.

(14) Baker, J. *J. Comput. Chem.* **1986**, *7*, 385.

(15) (a) Ziegler, T.; Rauk, A. *Theor. Chim. Acta* **1977**, *46*, 1. (b) Ziegler, T. In *Metal−Ligand Interactions: from Atoms, to Clusters, to Surfaces*; Salahub, D. R., Russo, N., Eds.; NATO ASI Series C378; Kluwer Academic: Dordrecht, The Netherlands, 1992. (c) Ziegler, T. *Chem. Rev.* **1991**, *91*, 651.

(16) (a) Snijders, J. G.; Baerends, E. J. *Mol. Phys.* **1978**, *36*, 1789. (b) Snijders, J. G.; Baerends, E. J.; Ros, P. *Mol. Phys.* **1979**, *38*, 1909.

(17) (a) Li, J.; Schreckenbach, G.; Ziegler, T. *Inorg. Chem.* **1995**, *34*, 3245. (b) Li, J.; Schreckenbach, G.; Ziegler, T. *J. Am. Chem. Soc.* **1995**, *117*, 486. (c) Li, J.; Schreckenbach, G.; Ziegler, T. *J. Phys. Chem.* **1994**, *98*, 4838.

Chart 1

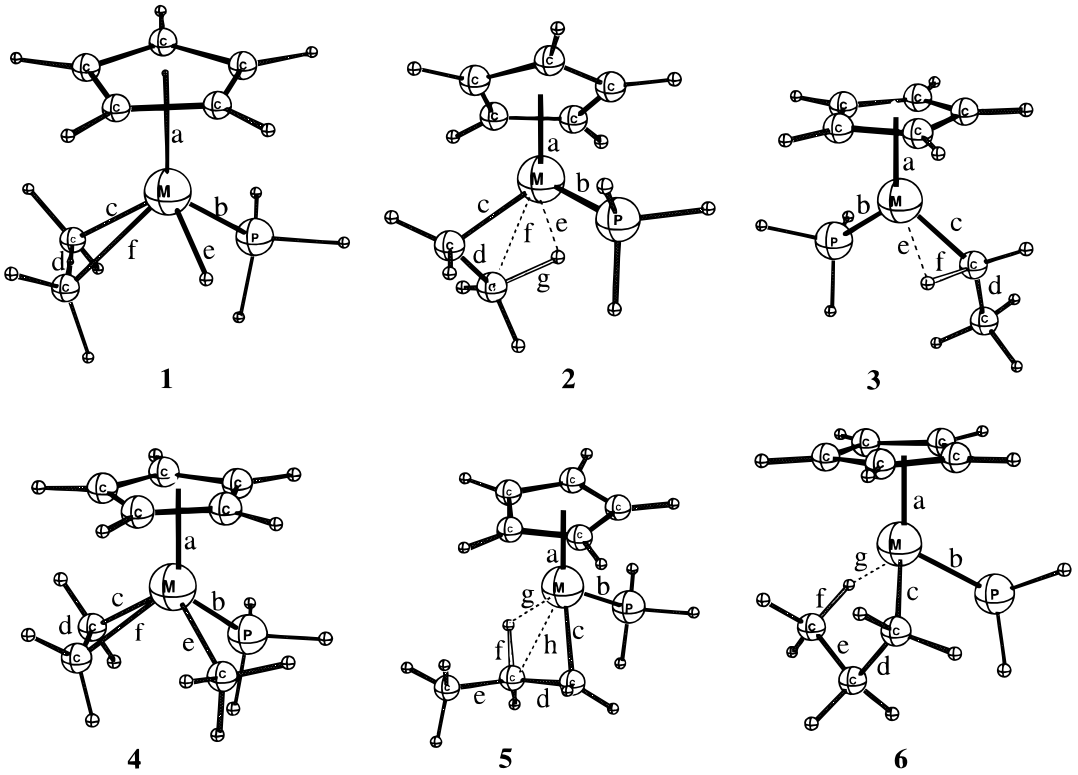

Table 1. Optimized Structures[a] of Olefin Hydrido and Ethyl Complexes

complexes	Co	Rh	Ir
1: $CpMPH_3(C_2H_4)H^+$ terminal			
a	1.644	1.878	1.986
b	2.102	2.222	2.256
c	2.016	2.109	2.171
d	1.395	1.391	1.394
e	1.454	1.581	1.590
f	2.016	2.110	2.163
cf	40.5	38.6	37.5
ef	73.0	73.2	71.7
2: $CpMPH_3C_2H_5^+$ β-H agostic			
a	1.631	1.851	1.954
b	2.117	2.207	2.261
c	1.942	2.208	2.089
d	1.450	1.449	1.455
e	1.575	1.699	1.796
f	2.053	2.184	2.282
g	1.267	1.248	1.236
cd	72.9	75.8	77.9
dg	113.8	113.1	113.7
eg	91.8	94.5	95.8
cdg	10.5	14.3	12.4
3: $CpMPH_3C_2H_5^+$ α-H agostic			
a	1.644	1.855	1.962
b	2.116	2.210	2.266
c	1.813	1.928	1.987
d	1.470	1.476	1.483
e	1.666	1.976	2.082
f	1.220	1.158	1.154
cd	134.6	130.5	130.4
ce	40.8	34.5	32.8
cf	63.1	75.0	78.1

[a] Bond distances (a, b, etc.) are in Å and bond angles (cd, ce, etc.) in deg. Distances and angles are labeled in **1**, **2**, and **3**, respectively.

of group-9 complexes with either a M−H or M−olefin bond. The reacting ethyl complex **2** with a β-agostic M−H−C bond can rearrange to the ethyl species **3**, which is stabilized by an α-H agostic interaction. The geometry of **3** is also given in Table 1, and the α-H agostic interaction is indicated by stretched C−H bonds (*f*) of 1.220, 1.158, and 1.154 for Co, Rh, and Ir, respectively. The C−H bond elongation in **3** is clearly smaller than in the β-agostic ethyl complex **2**, and we shall show in the next section that **3** is higher in energy than **2**.

Two stable key structures have been located on the potential energy surface for the methyl β-migratory insertion process of eq 2, Table 2. The first, **4**, represents the olefin methyl reactant of eq 2. The second, **5**, corresponds to the product, the propyl complex of eq 2 with a β-agostic M−H−C bond. Where comparable, the reactant complex **4** has geometrical parameters quite similar to those of the hydrido olefin complex **1**. Likewise, the comparable geometrical parameters in the two β-agostic alkyl complexes **5** and **2** are nearly matching, and the β-H agostic interaction in **5** results in considerably stretched C−H bonds (*f*) of 1.294 (Co), 1.282Å (Rh), and 1.268 Å (Ir), respectively. It is difficult to determine C−H distances in agostic M−H−C bonds accurately from experimental studies as the hydrogen is situated close to a large metal center.[18] However, the available experimental estimates[18] range from 1.1 to 1.3 Å. Theoretical studies[2e,i,j] typically give the C−H distances in the range 1.12 to 1.20 Å for early transition metals, and up to 1.3 Å for late transition metals.[2l] The C−H distances found in **2** and **5** are clearly indicative of strong agostic interactions.

The β-agostic complex **5** can rearrange to the γ-agostic propyl isomer **6**, which we shall show in the next section to be of higher energy than **5**. Judging from the relative C−H bond elongations in **5** and **6**, it seems clear that the former has a stronger agostic interaction between the C−H bond and the metal. This is also borne out by a comparison of the M−H distances in **5** and **6**. Finally, for each of the agostic structures **2**, **3**, **5**, and **6** we note that the agostic C−H bond is stretched the most in the case of cobalt. This would indicate that the 3d member of the triad

(18) (a) Brookhart, M.; Green, M. L. H.; Wong, L.-L. *Prog. Inorg. Chem.* **1988**, *36*, 1. (b) Brookhart, M.; Green, M. L. H. *J. Organomet. Chem.* **1983**, *250*, 395.

Table 2. Optimized Structures[a] of Olefin Methyl and Propyl Complexes

complexes	Co	Rh	Ir
4: $CpCo(PH_3)(C_2H_4)CH_3^+$			
a	1.660	1.884	1.995
b	2.102	2.192	2.260
c	2.038	2.116	2.165
d	1.390	1.391	1.395
e	2.013	2.071	2.118
f	2.019	2.103	2.150
be	79.4	78.8	77.6
cd	69.2	70.3	70.6
cf	40.1	38.5	37.7
ef	83.1	81.1	79.2
5: $CpCo(PH_3)C_3H_7^+$ (β-H agostic)			
a	1.634	1.855	1.958
b	2.110	2.203	2.260
c	1.947	2.035	2.091
d	1.448	1.446	1.451
e	1.497	1.499	1.499
f	1.294	1.282	1.268
g	1.555	1.668	1.759
h	2.070	2.188	2.284
bc	90.4	87.2	83.6
cd	73.8	75.8	78.0
cg	79.9	74.3	71.1
ch	42.1	39.8	33.5
cde	−110.3	−108.9	−110.8
6: $CpCo(PH_3)C_3H_7^+$ (γ-H agostic)			
a	1.653	1.868	1.976
b	2.114	2.201	2.245
c	1.975	2.037	2.088
d	1.497	1.497	1.499
e	1.515	1.519	1.516
f	1.175	1.155	1.159
g	1.676	1.842	1.936
bc	87.4	85.2	82.6
cd	94.6	98.3	99.9
cg	96.1	89.2	85.9
de	105.0	106.4	106.7
ef	115.6	114.6	114.4
fg	102.8	104.4	105.4
cde	−26.6	−25.0	−26.9

[a] Bond distances (a, b, etc.) are in Å and bond angles (cd, ce, cde, etc.) in deg. Distances and angles are labeled in **4**, **5**, and **6**, respectively.

Table 3. Relative Energies[c] of Species Involved in the Migratory Insertion Reactions

complexes	Co	Rh	Ir
$CpMPH_3(C_2H_4)H^+$ (**1**)	0.0	0.0	0.0
$CpMPH_3C_2H_5^+$ [a] (**2**)	−3.4	−1.0	3.7
$CpMPH_3C_2H_5^+$ [a] (**3**)	9.9	7.3	8.1
$CpMPH_3(C_2H_4)CH_3^+$ (**4**)	0.0	0.0	0.0
$CpMPH_3C_3H_7^+$ [b] (**5**)	−12.7	−8.5	−5.3
$CpMPH_3C_3H_7^+$ [b] (**6**)	−1.1	−1.9	1.2
TS1[a] (**10**)	0.3	2.7	6.1
TS2[b] (**11**)	15.2	19.8	23.2

[a] Relative to **1**. [b] Relative to **4**. [c] kcal/mol.

forms the strongest agostic bonds with the C−H linkage. We shall provide further evidence for this notion in the next section.

Thermochemistry. We shall now turn to a discussion of the thermochemistry for the two processes in eqs 1 and 2. Throughout reference is made to electronic energy differences without zero-point-energy corrections.

The relative energies of the species involved in the β-migratory insertion of ethylene into the metal−hydrogen bond, eq 1, are given in Table 3. We find that the β-agostic ethyl product **2** is more stable than the hydrido olefin reactant **1** by 3.4 and 1.0 kcal/mol for cobalt and rhodium, respectively, whereas **1** is more stable than **2** by 3.7 kcal/mol in the case of iridium. Brookhart et al.[4a,c] found experimentally that **2** is favored over **1** by 3−5 kcal/mol in the case of cobalt with our model PH_3 ligand replaced by various phosphines or olefins. The same authors observe that the energy difference between **1** and **2** is reduced further (<3 kcal/mol) in the case of rhodium and strongly dependent on the nature of the phosphine or olefin co-ligand. Experimental values are not available for the iridium systems. Our theoretical calculations provide the first quantitative support for the generally held notion[4,18] that hydrido olefin complexes are stabilized compared to the β-agostic alkyl isomers toward the heavier congeners in a triad of late transition metals. We shall shortly provide a rationale for this trend.

We note further that the α-agostic ethyl complex **3** was found to be 13.3 (Co), 8.3 (Rh), and 4.4 kcal/mol (Ir) above the β-agostic isomer in energy. These differences can be taken as a rough estimate (lower bound) for the strength of the β-agostic interaction, assuming that the corresponding α-agostic interactions are much weaker. The trend in the differences indicates further that cobalt forms a stronger M−H(b) bond than the heavier congeners, in line with the fact that the C−H linkage involved in the M−H(b) bond is stretched the most in the case of cobalt.

Table 3 affords the corresponding relative energies for the species involved in the β-migratory insertion of ethylene into the metal−methyl bond, eq 2. We find that the β-agostic propyl complex **5** as the product in eq 2 is more stable than the methyl olefin reactant **4** by 12.7 (Co), 8.5 (Rh), and 5.3 kcal/mol (Ir), respectively. Thus, in eq 2 the equilibrium is on the product side for all three metals. However, the relative stability of $CpM(PH_3)(C_2H_4)R^+$ compared to $CpM(PH_3)(CH_2CH_2R)^+$ is seen to increase down the triad for R = H as well as R = CH_3. Brookhart et al.[4a] have studied insertion processes similar to that of eq 2 in which methyl is replaced by ethyl. However, experimental reaction enthalpies were not reported.

The γ-agostic propyl isomer, **6**, was found to be 11.6 (Co), 6.6 (Rh), and 6.5 kcal/mol (Ir) higher in energy than **5**. Obviously, the M−H(g) agostic bond is weaker than the corresponding M−H(b) bond. It seems again that the M-H(b) agostic bond is especially strong for cobalt with the largest difference in energy between **5** and **6**. The M−H(b) agostic bond is primarily established by a donation of charge from the occupied σ_{CH} orbital to an empty d-based orbital on the metal, destabilized by antibonding interactions with the ligands. According to normal ligand field arguments, the destabilization[19] increases from 3d to 5d. Thus cobalt has the most suitable acceptor orbital, and the strongest β-agostic bond. Our ETS analysis confirmed that the cobalt center acted as the strongest acceptor. An α-agostic propyl isomer was not considered. It is likely less stable than **5** to the same extent as the α-agostic ethyl complex **3** is less stable than **2**.

We have performed a detailed thermochemical analysis of the calculated trends for the enthalpies of the processes in eqs 1 and 2. The analysis is based on bond dissociation energies for the reactions given in eqs 5 to 14.

$$\mathbf{1} \longrightarrow CpM(PH_3)H^+ + C_2H_4 \qquad D_5(M-C_2H_4) \quad (5)$$

$$CpM(PH_3)H^+ \longrightarrow CpMPH_3^+ + H^\bullet \qquad D_6(M-H) \quad (6)$$

$$\mathbf{2} \longrightarrow CpMPH_3^+ + C_2H_5^\bullet \qquad D_7(M-C_2H_5) \quad (7)$$

(19) the energies for the metal based LUMO's are −9.49 (Co), −9.02 (Rh) and −9.06 eV (Ir), respectively.

$$\mathbf{3} \rightarrow CpMPH_3^+ + C_2H_5^\bullet \qquad D_8(M-C_2H_5) \qquad (8)$$

$$\mathbf{4} \rightarrow CpM(PH_3)CH_3^+ + C_2H_4 \qquad D_9(M-C_2H_4) \qquad (9)$$

$$CpM(PH_3)CH_3^+ \rightarrow CpM(PH_3)^+ + CH_3^\bullet \qquad D_{10}(M-CH_3) \qquad (10)$$

$$\mathbf{5} \rightarrow CpMPH_3^+ + C_3H_7^{\bullet +} \qquad D_{11}(M-C_3H_7) \qquad (11)$$

$$\mathbf{6} \rightarrow CpMPH_3^+ + C_3H_7^{\bullet +} \qquad D_{12}(M-C_3H_7) \qquad (12)$$

$$CH_3CH_2^\bullet \rightarrow C_2H_4 + H^\bullet \qquad D_{13}(H-CH_2CH_2^\bullet) \qquad (13)$$

$$CH_3CH_2CH_2^\bullet \rightarrow C_2H_4 + CH_3^\bullet \qquad D_{14}(CH_3-CH_2CH_2^\bullet) \qquad (14)$$

All bond dissociation energies defined in eqs 5 to 12 are shown in Table 4. We have in addition calculated that $D_{13}(H-CH_2-CH_2^\bullet) = 42.7$ kcal/mol and $D_{14}(CH_3-CH_2CH_2^\bullet) = 25.8$ kcal/mol. The fact that the C−C bond is weaker than the C−H bond is generally attributed[20] to a stabilization of the methyl radical as it attains a planar conformation (4 kcal/mol) as well as a larger steric interaction between $R^\bullet$ and C_2H_4 in $RCH_2-CH_2^\bullet$ for R = CH_3 compared to R = H. The structures of $CpM(PH_3)^+$ (**7**), $CpM(PH_3)H^+$ (**8**), and $CpM(PH_3)(CH_3)^+$ (**9**) were also fully optimized. The methyl complex **9** exhibits a clear α-H agostic interaction.

The enthalpy for the β-migratory insertion, **1** → **2**, of ethylene into the metal−hydrogen bond, eq 1, is given by

$$\Delta H_1 = D_6(M-H) + D_5(M-C_2H_4) - D_7(M-C_2H_5) - D_{13}(H-CH_2CH_2^\bullet) \qquad (15)$$

In the β-migratory insertion process, **1** → **2**, we form a carbon−hydrogen bond, $D_{13}(H-CH_2CH_2^\bullet)$, which has the same energy for all three metals, as well as a metal−ethyl bond which happens to be of similar strength, $D_7(M-C_2H_5)$, for M = Co, Rh, and Ir, Table 4. Thus, the trend in ΔH_1 will be set by changes in the energy required to break the metal−hydrogen, $D_6(M-H)$, and metal−ethylene, $D_5(M-C_2H_4)$, bonds, eq 15. We note that the metal−hydrogen bond strength, $D_6(M-H)$, increases considerably down the triad. This is in part due to the usual[21] relativistic stabilization of σ-bonds involving 4d and (in particular) 5d elements, Table 4. On the other hand, the metal−ethylene bond energy $D_5(M-C_2H_4)$ is seen to follow the opposite trend. Our ETS analysis indicates that the stronger $Co-C_2H_4$ bond is due to the better acceptor ability of cobalt, just as in the case of the β-agostic M−H(b) interaction.

Combined $D_5(M-C_2H_4) + D_6(M-H)$ increases down the triad to the extent where ΔH_1 becomes positive for iridium so that the hydrido ethylene isomer, **1**, is more stable than the β-agostic, **2**, ethyl complex. For cobalt, the metal−hydrogen bond is too weak to favor **1** over **2** whereas $D_6(M-H)$ is large enough for rhodium to make **1** and **2** similar in energy with $\Delta H_1 = -1.0$ kcal/mol, Table 3. It is perhaps surprising that the corresponding metal−ethyl bond energy $D_7(M-C_2H_5)$, in contrast to $D_6(M-H)$, is quite similar for all three metals. The explanation here is that the removal of an ethyl group from **2** breaks not only a metal−carbon σ-bond but also a β-agostic M−H(b) bond. The latter decreases (as argued before) in strength from cobalt to iridium, while the former increases. That the pure carbon−metal σ-bond in fact ought to increase down the triad is evident from the calculated values of $D_{10}(M-CH_3)$, Table 4.

Table 4. Calculated Bond Disociation Energies[a,b]

eq no[c]	bond energy	Co	Rh	Ir
5	$D_5(M-C_2H_4)$	36.1(0.5)	30.3(1.7)	30.3(2.2)
6	$D_6(M-H)$	60.0(0.8)	67.4(3.0)	72.6(8.3)
7	$D_7(M-C_2H_5)$	56.9(1.0)	56.1(3.2)	56.5(5.6)
8	$D_8(M-C_2H_5)$	43.4(1.2)	47.7(3.6)	52.0(8.9)
9	$D_9(M-C_2H_4)$	27.1(0.1)	24.3(1.2)	24.1(11.5)
10	$D_{10}(M-CH_3)$	43.9(1.2)	49.9(3.0)	54.7(9.3)
11	$D_{11}(M-C_3H_7)$	57.7(1.1)	56.9(3.4)	58.6(5.9)
12	$D_{12}(M-C_3H_7)$	46.4(0.8)	50.3(2.8)	51.9(6.4)

[a] kcal/mol. [b] Relativistic contributions in parentheses. [c] Numbers refer to eqs 5−12 defined in the text.

The enthalpy for the β-migratory insertion, **4** → **5**, of ethylene into the metal−methyl bond, eq 2, is given by

$$\Delta H_2 = D_{10}(M-CH_3) + D_9(M-C_2H_4) - D_{11}(M-C_3H_7) - D_{14}(CH_3-CH_2CH_2^\bullet) \qquad (16)$$

where **5** is the propyl product with the β-agostic M−H(b) bond. In the β-migratory insertion process, **4** → **5**, we form a metal−propyl bond with a strong β-agostic component and a strength, $D_{11}(M-C_3H_7)$, that is almost identical with that, $D_7(M-C_2H_5)$, of the metal−C_2H_5 bond in the β-agostic ethyl product of eq 1. On the other hand, the carbon−carbon bond formed, $D_{14}(CH_3-CH_2CH_2^\bullet) = 25.8$ kcal/mol, is (as already discussed) considerably weaker than the analogous C−H bond, $D_{13}(H-CH_2CH_2^\bullet) = 42.7$ kcal/mol, generated in eq 1. However, this is compensated for by the fact that the breakage of a $M-CH_3$ linkage requires accordingly less energy,[20] $D_{10}(M-CH_3)$, than the rupture of the M−H bond, $D_6(M-H)$, in eq 1. Thus, the only factor left to make ΔH_2 significantly different from ΔH_1 is the metal−ethylene dissociation energy. We find, Table 4, that the $M-C_2H_4$ bond is weaker in **4**, $D_9(M-C_2H_4)$, than in **1**, $D_5(M-C_2H_4)$, with the result that the β-migratory insertion process, **4** → **5**, is calculated to be exothermic for all three metals, Table 3. The $M-C_2H_4$ bond is weakened in **4** compared to **1** due to an increase in the steric interaction as the hydride ligand is replaced with a methyl group. The increase in steric bulk is particularly felt for cobalt with the shortest metal−ligand bond distances.

Kinetics. We have fully optimized the transition states for the β-migratory insertion reactions of eqs 1 and 2. The optimized structures **10** and **11** were confirmed to have a single imaginary frequency. Their geometries (key parameters) are given in Table 5.

Transition state **10** corresponds to the insertion of olefin into the metal−hydrogen bond, eq 1 For cobalt and rhodium the transition state **10** is reactant-like with M−H bond distances of 1.459 and 1.574 Å, respectively, close to those found in the terminal hydride complex **1**. On the other hand, the transition state for iridium is seen to be product-like with an Ir−H bond distance of 1.869 Å, closer to the Ir−H bond length in the β-agostic ethyl product, **2**. These trends are in line with eq 1 being endothermic for M = Co, Rh and exothermic for M = Ir. The structures of **10** clearly indicate that the β-migratory insertion reactions eq 1 for all three metals proceed via a four-center transition state. The calculated barriers for the β-migratory insertion reaction 1 are 0.3 (Co), 2.7 (Rh), and 6.1 kcal/mol (Ir), respectively, Table 3. Thus, the activation energy increases as the insertion reaction becomes thermodynamically less favorable.

(20) Bickelhaupt, F. M.; Ziegler, T.; Schleyer, P. v. R. *Organometallics* **1996**, *15*, 1477.
(21) Ziegler, T.; Tschinke, V.; Becke, A. *J. Am. Chem. Soc.* **1987**, *109*, 1351.

Table 5. Geometries of Transition States[a]

complexes	Co	Rh	Ir
TS1 (**10**)			
a	1.641	1.864	2.000
b	2.109	2.202	2.346
c	1.996	2.075	2.159
d	1.406	1.414	1.458
e	1.459	1.574	1.869
f	2.014	2.125	2.366
g	1.726	1.562	1.218
cd	70.2	72.7	79.1
dg	110.8	112.5	113.8
eg	77.9	85.3	97.8
cdg	16.7	18.6	12.0
TS2 (**11**)			
a	1.686	1.914	2.012
b	2.149	2.284	2.335
c	1.963	2.091	2.164
d	1.441	1.428	1.428
e	2.171	2.298	2.386
f	2.133	2.302	2.396
g	1.884	1.967	1.990
cd	75.9	79.3	80.8
dg	121.9	121.7	122.9
cdg	−29.6	−28.8	−27.3

[a] Bond distances (a, b, etc.) are in Å and bond angles (cd, ce, cdf, etc.) in deg. Distances and angles are labeled in **10** and **11**, respectively.

Chart 2

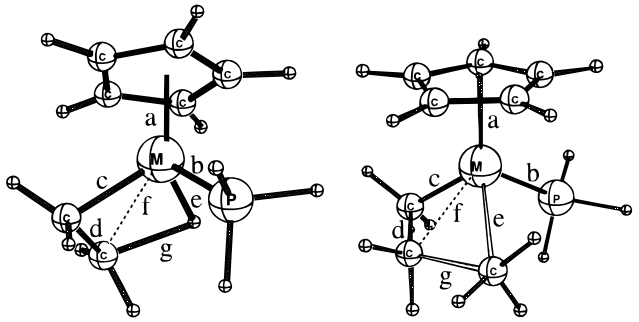

10 **11**

Brookhart et al. have carried out kinetic experiments for cobalt[4c] and rhodium[4a] with some bearings on our calculated activation energies for the β-migratory insertion reaction 1. They observed the process **12a** → **12e** of eq 17:

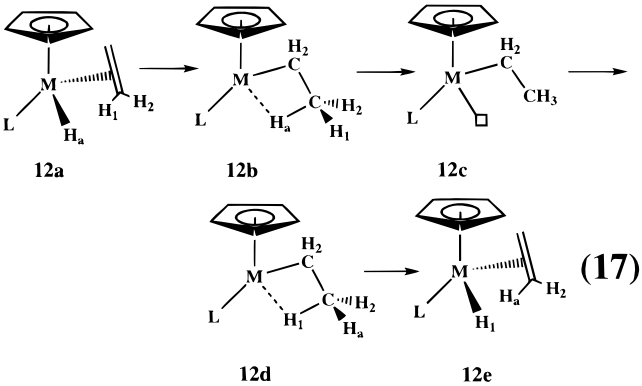

12a **12b** **12c**

12d **12e** **(17)**

in which the metal hydrogen, H_a, is exchanged with hydrogens on the same olefin carbon, H_1 and H_2. They recorded the energy barrier $\Delta H_{20}^{\ddagger}$, which they termed activation energy for hydride insertion. However, the experimental $\Delta H_{20}^{\ddagger}$ values are only directly comparable to our activation barriers if the insertion step **12a** → **12b** is much slower than the step **12b** → **12c** in which H_a, H_1, and H_2 are equilibrated. As already pointed out by Brookhart et al.,[4a] this is not the case since the latter process seems to be rate limiting in eq 17. Thus it is not surprising that experimental $\Delta H_{20}^{\ddagger}$ values are larger than our estimates for the activation energies of the β-migratory insertion reaction 1. In fact, a lower bound estimate for the barrier in the equilibration step **12b** → **12c** would be the difference in energy, $\Delta H_{2\rightarrow 3}$, between the β-agostic ethyl complex **2** and its α-agostic isomer **3**. Both $\Delta H_{20}^{\ddagger}$ and $\Delta H_{2\rightarrow 3}$ are in the range of 8−12 kcal/mol.

Transition state **11** corresponds to the insertion of ethylene into the metal−methyl bond eq 2. The transition state **11** is reactant-like for all three metals, in accordance with the exothermic nature of eq 2. Thus, compared to the reactant **4**, the C−C bond (d) is stretched by less than 0.05 Å and the M−CH_3 bond (e) is elongated by up to 0.25 Å. Further, the emerging C−C bond (g) is still some 0.40 Å longer than a normal single C−C bond. There is no α-agostic interaction present in **11**.

The calculated barriers of 15.2 (Co), 19.8 (Rh), and 23.2 kcal/mol (Ir) are all higher than in eq 1 and exhibit an increase down the triad as the insertion becomes thermodynamically less favorable. Our estimates are in good agreement with the experimental value[4c] of 14.3 kcal/mol for the migratory insertion of ethylene into the Co−ethyl bond in $(\eta^5\text{-}C_5Me_5)CoP(OMe)_3(C_2H_4)CH_2CH_3^+$ and the value[4a] of 22.4 kcal/mol for the corresponding migratory insertion process in the homologous rhodium compound $(\eta^5\text{-}C_5Me_5)RhP(OMe)_3(C_2H_4)CH_2CH_3^+$. Tentative[4a] experimental measurements found the insertion barrier of ethylene into the metal−methyl bond to be 1 kcal/mol higher. No experimental values have been reported in the case of iridium.

It is perhaps surprising that the migratory insertion of hydride, eq 1, has a lower barrier than the migratory insertion of methyl, eq 2, as the metal−hydrogen bond is stronger than the metal−methyl bond. This can be rationalized[2f,m,n,3f] by observing that the barrier in eq 1 stems from the destabilization of the electron pair **13a**, as the hydrogen moves from the metal toward the olefin carbon. Initially the electron pair is located in the M−H σ-bonding orbital. As the hydrogen moves from the metal toward the nearest olefin carbon, the bonding overlap between $1s_H$ and the metal σ orbital is reduced. However, during the move, the spherical $1s_H$ orbital can make up for the loss in stabilizing interaction with the metal s orbital by interacting with the in-phase lobe of the π^* ethylene orbital. Thus the ability of the spherical $1s_H$ orbital to interact throughout the reaction with both the metal and carbon center substantially reduces the barrier. The same type of destabilization, **13b**, occurs in the migratory insertion of methyl, eq 2. However, the CH_3 orbital is more directional[2f,m,n,3f] and less able to interact with the metal s orbital and the in-phase lobe of the π^* ethylene orbital at the same time, **13b**, as it changes its direction from pointing toward the metal to directing its lobe at the ethylene carbon. As a result the barrier in eq 2 is higher.

The migratory insertion of alkyls, $L_nM(C_2H_4)R \rightarrow L_nMC_2H_4R$, seems to be both thermodynamically and kinetically more favorable for early transition metals[2g,i−k,m,3g] and f-block elements[3a,e] than for late to middle transition metals.[2f,h,l,3d,4] In the olefin alkyl reactant $L_nM(C_2H_4)R$ the π^* olefin orbital will form bonding, **14a**, and antibonding, **14b**, interactions with a d_π metal orbital. For d^0 systems both **14a** and **14b** are empty. Thus, the stabilization of the reactant from the metal d_π to olefin π^* back-donation, **14a**, is lacking, and the insertion is thermodynamically relatively facile. Further, in the d^0 systems the unoccupied in-phase combination of low energy, **14a**, is available to act as the π^* acceptor orbital in **13b** when the methyl group migrates toward the olefin carbon. This will help

Chart 3

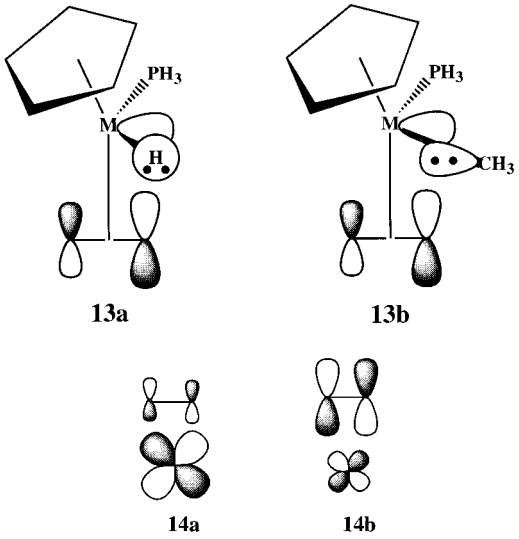

13a **13b**

14a **14b**

in lowering the barrier as much as possible. In the middle to late transition systems **14a** is occupied and $L_nM(C_2H_4)R$ stabilized by metal d_π to olefin π^* back-donation. This makes the insertion thermodynamically less favorable. Also, only the **14b** orbital of high energy can initially act as acceptor orbital in **13b**, which will increase the barrier.

Concluding Remarks

We have studied the migratory insertion of ethylene into the M−H and M−CH$_3$ bonds in CpM(PH$_3$)(CH$_2$CH$_2$)R$^+$ (R = H, CH$_3$; M = Co, Rh, Ir). Hydride migration eq 1 is exothermic for cobalt ($\Delta H_e = -3.4$ kcal/mol) and rhodium ($\Delta H_e = -1.0$ kcal/mol), but endothermic for iridium ($\Delta H_e = 3.7$ kcal/mol). The corresponding reaction barriers for eq 1 are 0.3 (Co), 2.7 (Rh), and 6.1 kcal/mol (Ir), respectively. The reaction 1 becomes kinetically and thermodynamically less favorable down the triad as the metal−hydrogen bond strength increases due to relativistic effects. Methyl migration is exothermic for all three metals with $\Delta H_e = -12.7$ (Co), −8.5 (Rh), and −5.3 kcal/mol (Ir), respectively. The corresponding reaction barriers are 15.2 (Co), 19.8 (Rh), and 23.2 kcal/mol (Ir), respectively. Again the reaction 2 becomes kinetically and thermodynamically less favorable down the triad as the metal−methyl bond strength increases due to relativistic effects. Migration is thermodynamically more favorable for methyl because the methyl olefin complex, **4**, has a weaker metal−ethylene bond. On the other hand, hydride migration is kinetically more favorable as the spherically symmetric $1s_H$ orbital, **13a**, is better able to stabilize the transition state than the directional σ_{CH_3} orbital of the methyl group, **13b**. The alkyl products **2** and **5** are both stabilized by agostic interactions between the metal and a β-hydrogen on the alkyl group. The agostic interaction decreases toward the heavier element in the cobalt triad.

Acknowledgment. This investigation was supported by the Natural Science and Engineering Research Council of Canada (NSERC). We would like to thank the Petroleum Research Fund administered by the American Chemical Society (ACS-PRF No. 31205-AC3) for further support of this research. A Canada Council Killam research fellowship to T.Z. is also acknowledged.

Supporting Information Available: Optimized geometrical parameters are available for structures **7**, **8**, and **9** (4 pages). See any current masterhead page for ordering and Internet access instructions.

JA9700156